https://doi.org/10.5194/egusphere-2026-2050
Preprint. Discussion started: 15 April 2026

In-Situ and Remote Observations of the Ring Current and Radiation Belt during JUICE Lunar Earth Gravity Assist

Pontus C. Brandt[1], George Clark[1], Donald G. Mitchell[1], Peter Kollmann[1], Matina Gkioulidou[1], Leonardo Regoli[1], Kostas Dialynas[2], Frederic Allegrini[3], Nicolas Andre[4], Xianzhe Jia[5], Krishan Khurana[6], Carol Paty[7], Stanislav Barabash[8], Peter Wurz[9]

[1]The Johns Hopkins University Applied Physics Laboratory, Laurel, MD, USA
[2]Academy of Athens, Athens, Greece
[3]Southwest Research Institute, San Antonio, TX, USA
[4]Institut de Recherche en Astrophysique et Planétologie, Toulouse, France
[5]University of Michigan, Ann Arbor, MI, USA
[6]University of California Los Angeles, Los Angeles, CA, USA
[7]University of Oregon, Eugene, OR, USA
[8]Swedish Institute of Space Physics, Kiruna, Sweden
[9]University of Bern, Bern, Switzerland

Correspondence to: Pontus C. Brandt (pontus.brandt@jhuapl.edu)

Abstract. This report presents an overview of the observations and performance of the Jovian Energetic Neutrals and Ions (JENI) and the Jovian Energetic Electrons (JoEE) belonging to the Particle Environment Package (PEP) onboard the Jupiter Icy Moon Explorer (JUICE) during its Lunar-Earth Gravity Assist (LEGA) 19-23 August 2024. Observations from the Lunar and Earth flybys are presented and discussed. While the environment around the Moon was very quiet, the Earth flyby presented a characteristic, nearly symmetric recovery phase ring current with adiabatically increasing energies with decreasing distance to Earth, and butterfly pitch-angle distributions (PADs) at high L-shells transitioning to distributions rounded around 90˚ pitch angle at lower L-shells. The electron radiational belt showed a double-structured outer zone, possibly from a fresh intensification, and the characteristic slot region created by loss through interactions with plasmaspheric hiss. On the outbound, JENI was operated as an Energetic Neutral Atom (ENA) camera and observed the energetic ions of the inner magnetosphere from 17.4 R_E to 150 R_E. During this period multiple intensifications were observed in the night side magnetosphere consistent with substorm injections. The LEGA observations provided useful data for further calibrating the sensors that overall showed a nominal performance.

1 Introduction

The Jovian Energetic Neutrals and Ions (JENI) and the Jovian Energetic Electrons (JoEE) are two energetic particle instruments belonging to the Particle Environment Package (PEP) onboard the Jupiter Icy Moon Explorer (JUICE). Together, JENI and JoEE are referred to as PEP-Hi and is a NASA-funded contribution to JUIC, led by The Johns Hopkins Universty Applied Physics Laboratory. While JENI is a combined in-situ ion spectrometer and a remote Energetic Neutral Atom (ENA) camera, and JoEE is an in-situ energetic electron spectrometer.

https://doi.org/10.5194/egusphere-2026-2050
Preprint. Discussion started: 15 April 2026

Launched on 23 April 2023, JUICE is now in cruise to Jupiter, where it will arrive in 2031. Between 19 and 23 August 2024, the JUICE spacecraft conducted a retrograde Lunar and Earth Gravity Assist (LEGA) to line up its trajectory for a later prograde Venus Gravity Assist. During this period PEP-Hi observed the near-lunar space environment deep in the terrestrial magnetotail with a lunar closest approach at 21:16 UTC on 19 August 2024, and the inner magnetosphere of Earth, with a closest approach at 21:57 UTC on 20 August 2024. After crossing the terrestrial magnetopause on the outbound trajectory, JENI remotely observed the terrestrial ring current in ENAs for several days while JoEE measured the in-situ energetic electron environment in the solar wind.

In this brief report, we present the PEP-Hi observations and performance during the entire LEGA period. Section 2 provides an overview of the JENI and JoEE. Section 3 presents the observations near the Moon, the in-situ measurements through the terrestrial plasma sheet, ring current and radiation belt, and the remote ENA observations of the ring current and plasma sheet during the outbound trajectory. The outbound ENA observations by JENI and the radiation belt measurements by JoEE are described in depth in the papers by Gkioulidou et al. (2026) and Clark et al. (2026)

2 Instruments

PEP (Figure 1) consists in total of six instruments measuring ions, electrons, ENAs, neutral gas, over a comprehensive energy and composition range. See Barabash et al. (2026) for detailed review of the instrument suite. In addition to PEP-Hi, the Jovian plasma Dynamics and Composition (JDC) measures the distribution of positive and negative ions in the ~1 eV – 42 keV range; the Jovian Electrons and Ions (JEI) measures electrons in the ~1 eV – 55 keV range and is also capable of measuring total ions; the Neutral gas and Ion Mass spectrometer (NIM) measures neutral gas and thermal plasma composition over the 1-1000 amu range; the Jovian Neutrals Analyzer (JNA) remotely detects low-energy ENAs in the ~10 eV – 3 keV.

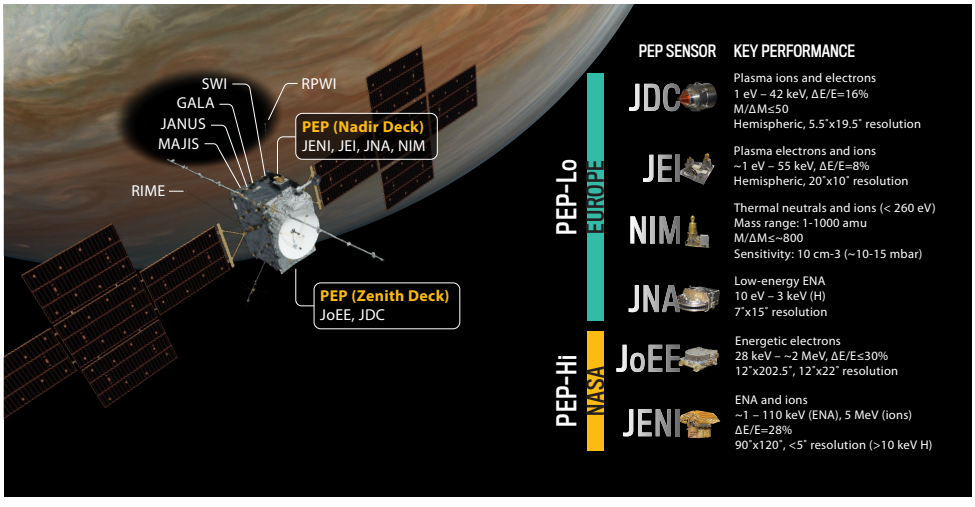

Figure 1: Overview of PEP on the JUICE spacecraft.

https://doi.org/10.5194/egusphere-2026-2050
Preprint. Discussion started: 15 April 2026

Table 1: Performance Table of JoEE and JENI

JENI	
Energy range	1 – 110 keV (ENAs)
	1 keV – 5 MeV (ions)
	30 - 300 keV (electrons)
Energy Resolution, $\Delta E/E$	≤28% (≥ 30 keV He)
	<30% (≥30 keV electrons)
Masses resolved	H, He, O, S
FOV	≥92°x120.6° (MCPs)
	≥70°x120° (SSDs)
Angular Resolution	≥2.5˚
Geometric Factor	0.001 - 1.85 cm^2 sr
Grid Transmission	~0.3
JoEE	
Energy Range	~28 keV - 2 MeV (electrons)
	~325 keV – 1.2 MeV (ions)
Energy Resolution, ΔE/E	< 30 % for ≥ 30 keV electrons
FOV	180˚ x 12˚
Angular Resolution	22.5˚
Geometrical Factor	0.00505 cm^2 sr (per pixel)

2.1 Jovian Energetic Neutrals and Ions

JENI is a combined ion and ENA camera based on its predecessors, the High-Energy Neutral Atom (HENA) camera (Mitchell et al. 2000) on board the IMAGE mission and the Ion Neutral Camera (INCA) (Krimigis et al. 2004) on board the Cassini mission. JENI consists of two assemblies of deflection blades that filter out charged particles when high voltage is applied across the blades and therefore enables JENI to image ENAs. Once a particle has passed through the deflection assembly it enters one of two slits with a variable aperture size. Here, the particle penetrates a start foil mounted directly beneath the aperture. Electrons released as the particle passes through the foil are steered to a micro-channel plate (MCP) detector that records the start position (along the slit) and start time of the particle. Next, the particle impacts a two-dimensional stop plane where the stop time and position of the particle is recorded. The resulting 1D and 2D start and stop positions determine the particle direction and the difference between the two start and stop timing pulses determine the time-of-flight (TOF) of the particle. Particle mass can be determined in two ways: The stop plane consists of a larger MCP area

https://doi.org/10.5194/egusphere-2026-2050
Preprint. Discussion started: 15 April 2026

and a smaller solid-state detector (SSD). If the particle impacts the stop MCP, the mass can be estimated through the pulse height (PH) of the electron pulse on the backside of the MCP. If the particle impacts the SSD, the resulting measured energy deposition can be combined with the TOF to more accurately resolve, H, He, O and S. We refer to these two data products as TOFxPH and TOFxE. As the particle penetrates a stop foil mounted over the stop plane electrons are generated on the front of the foil and are steered to coincidence MCP that records a third temporal and spatial pulse. These additional pulses provide further spatial and temporal coincidences that are effective in reducing the UV and penetrating backgrounds.

2.2 Jovian Energetic Electrons

JoEE is a circular, multi-directional, compact electron spectrometer and consists of nine angular sectors that each holds three SSDs and magnets in a spoke-like configuration to create a circular, and relatively closed magnetic field around spectrometer. As an electron enters a sector, the magnetic field deflects the electron to one of the three SSDs depending on its energy. This magnetic selection also acts as an extra coincidence measurement that is used to reject unwanted background. Three of the nine sectors have SSD assemblies mounted perpendicular to the circular plane and parallel to the boresight of the sector. These three SSD assemblies detect electrons whose energy is too high to affect their trajectories appreciably. Each assembly consist of a stack of three SSD wafers to determine the electron energy while imposing criteria on the energy deposited in each wafer to reject background.

3 Observations

As depicted by the black line in Figure 2, JUICE approached the Moon and Earth from the anti-sunward side, almost entirely in the ecliptic plane and entered the terrestrial magnetotail around 200 Earth radii (R_E) downstream of Earth. The Lunar CA occurred at 21:16 UTC at an altitude of 755 km on 19 August 2024 and Earth CA at 21:57 UTC at an altitude of 6807 km on 20 August 2024. The yellow and blue comet-like curves represent the magnetopause distance at a 4 nPa pressure balance with the solar wind dynamic pressure and a typical bowshock distances, respectively. The green line indicate the position of the Moon the blue dot is Earth. JUICE first performed a lunar gravity assist to almost perfectly align the trajectory with the Sun-Earth line and was followed by a flyby of Earth on its dawn side for a retrograde gravity assist (resulting in decreased speed) to align the trajectory for the later prograde Venus gravity assist. In a relatively short period around lunar flyby JENI was switched on in its ENA mode to attempt ENA imaging of the lunar surface and its interaction with the plasma flows in the magnetotail. JoEE was on in its standard science mode to measure any energetic electrons in the near-lunar space environment. After the lunar observations, JoEE remained on and JENI was switched to ion mode and remained in that mode throughout the traversal of the magnetosphere. After exiting the magnetosphere, JoEE remained on and JENI was switched back to ENA mode as the spacecraft slewed to acquire Earth near the center of JENI's large FOV offering excellent viewing of the inner magnetosphere for several days as JUICE left Earth.

https://doi.org/10.5194/egusphere-2026-2050
Preprint. Discussion started: 15 April 2026

During this entire period the interplanetary magnetic field (IMF) displayed only weak fluctuations north- and southward of a few nT. The SYMH index was therefore only -10 nT at most with no geomagnetic storm developing. However, the AE and AL indices displayed auroral substorm activity. Note also that a week prior to LEGA, the Earth was impacted by a relatively significant CME causing a geomagnetic storm of peak SYMH magnitude of -188 nT. Below we now report on the observations in more detail.

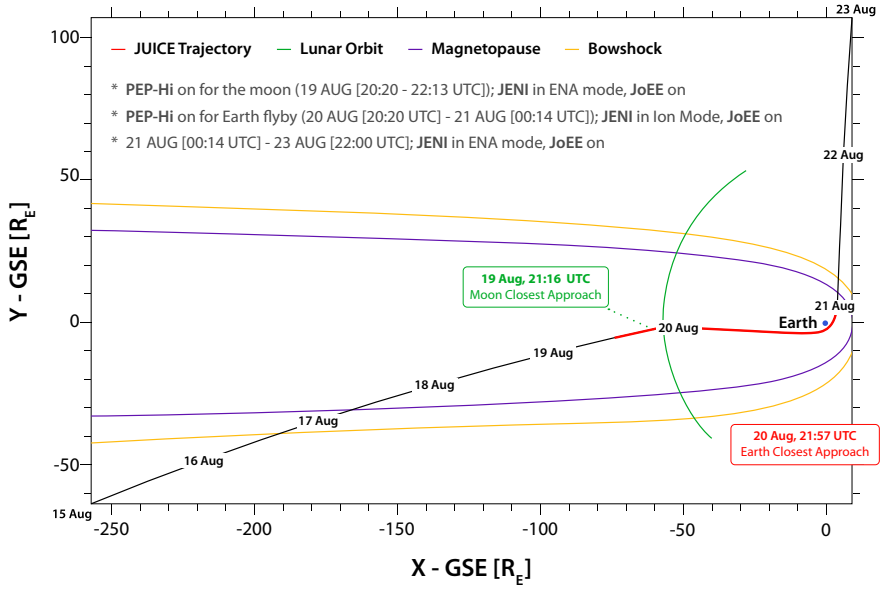

Figure 2: Overview of LEGA trajectory.

3.1 Observations Near the Moon

The observation period of JENI and JoEE near the Moon began at around 20:20 UTC on 19 August 2024 and ended at 22:13 UTC on that same day. The Moon entered JENI's FOV at around 20:59 UTC and began to view the sunlit lunar side at 21:14 UTC. The Moon exited JENI's FOV at 22:09 UTC and PEP-Hi was turned off shortly thereafter. During this time JENI attempted to detect any ENAs originating from energetic ions bombarding the lunar surface and backscattered as neutrals. Such as signal was detected as predicted (Futaana et al. 2006) when the Moon was immersed in the much more intense solar wind by Chandrayaan (Vorburger et al. 2013; Wieser et al. 2010; Wieser et al. 2009; Schaufelberger et al. 2011) and by the Interstellar Boundary Explorer (McComas et al. 2009). However, the ambient ion intensities as measured simultaneously by JDC were very weak and no ENA signal could be detected in the JENI observations. Similarly, the energetic electron environment probed by JoEE near the Moon was also near detection threshold. Note that JoEE was designed for the much harsher radiation environment and higher electron intensities at Jupiter.

https://doi.org/10.5194/egusphere-2026-2050
Preprint. Discussion started: 15 April 2026

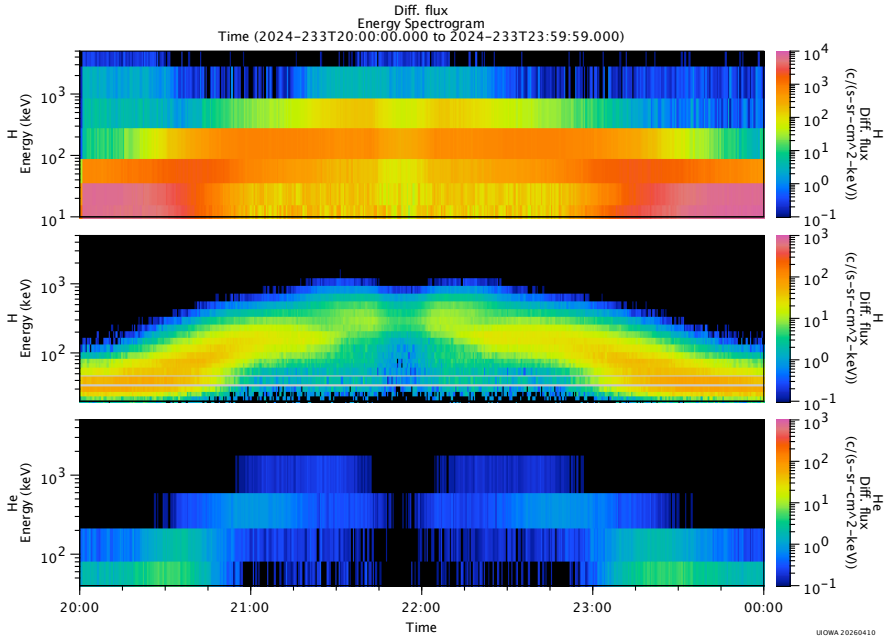

Figure 3: JENI in-situ ion measurements in the ring current. (a) Proton intensities integrated over all measured pitch angles using TOFxPH, (b) same as (a), but using TOFxE, (d) same as (c), but for He^+.

3.2 In-Situ Measurements of the Terrestrial Magnetosphere

At 17:57 UTC on 20 August 2024 at a distance of about 15 R_E downtail, JoEE turned back on its standard science mode and JENI was turned on in ion mode with the aperture in the single pin-hole position. Figure 3 shows the JENI data products starting around 20:00 UTC on 20 August 2024 through the ring current showing (a) the proton energy-time spectrogram for all directions obtained using the TOFxPH technique, (b) the proton spectrogram for all directions obtained using the TOFxE technique, and (c) is the same as (b) but for He^+. The data products of the TOFxE spectrograms in Figures 3b and 3c were created by binning the counts in TOF - energy (TOFxE) space and is depicted in Figure 4. Here, we see the corresponding individual counts ("events") in TOF by energy space integrated over 20:00 to 00:00 UTC with the predefined energy and species bins overlaid. See Barabash et al. (2026) for a definition of the bins. The counts show the two distinct tracks of protons (lower track) and He^+ (upper track). The O^+ bins are located directly above the He^+ bins and there is no discernable track of O^+ counts as expected for a recovery phase ring current where O^+ ions are lost first due to their shorter lifetime against charge exchange with geocoronal H. Based on previous studies, the expected ratio of O^+ to proton intensity is on the order of 0.01 or less (Gloeckler et al. 1985; Hamilton et al. 1988; Nosé et al. 2005).

The observation period in Figure 3 begins at around 20:00 UTC when JUICE is already in the ring current. The upper TOFxPH spectrogram in Figure 3a shows the predominant low-energy population in the outer ring current between 20:00-

https://doi.org/10.5194/egusphere-2026-2050
Preprint. Discussion started: 15 April 2026

20:30 UTC, which likely also contains a mix of protons and He^+ for this data product. After this period, intensities are dominated by more energetic protons.

All of the ion spectrograms show the characteristic intensification and energization of ions all the way into closest approach. This is a representative behavior of the so-called ring current, where the ion energization and intensification is dominated by conservation of the first adiabatic invariant as ions have both been injected into and drifted inward to lower L-shells by the ExB drift. The minimum in intensities around 21:45-22:00 UTC, is consistent with the inner edge of the ring current. The higher resolution TOFxE proton spectrum in Figure 3b display some structure with enhanced intensity regions around 21:30-21:45 UTC and similar on the outbound leg around 22:00-22:15 UTC. This structure could be a remnant from an older ring current population, with a younger population outside of it generated by more recent disturbances in the solar wind. All ion spectrograms appear nearly symmetric around Earth CA, which indicates that this could be a near-symmetric ring current created from a past larger geomagnetic storm that trapped ions on closed drift paths.

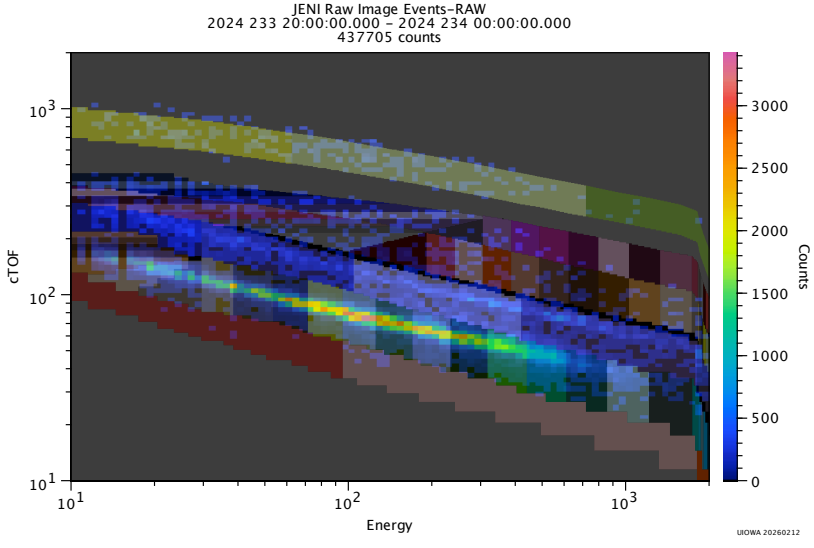

Figure 4: JENI TOFxE single-ion ("event") measurements integrated over the entire ring current traversal from 20:00 to 00:00 UTC and integrated over all measured pitch angles. The overlaid bins show the composition and energy bins defined in the onboard software to create the energy spectra for each species (see Figure 3). The lower and most intense band is protons and the fainter band just above it is He^+. The O^+ bins above the He^+ bins contain almost no counts.

Figure 5 shows the proton PADs for a sample of energies starting with (a) 23 keV, (b) 55 keV, (c) 152 keV, and (d) 478 keV. All energies show butterfly distributions at the outer L-shells that transition to PADs rounded around 90˚ further in. This is characteristic of the recovery phase ring current and is due to drift-shell splitting at high L-shells and magnetopause shadowing (Shi et al. 2016).

https://doi.org/10.5194/egusphere-2026-2050
Preprint. Discussion started: 15 April 2026

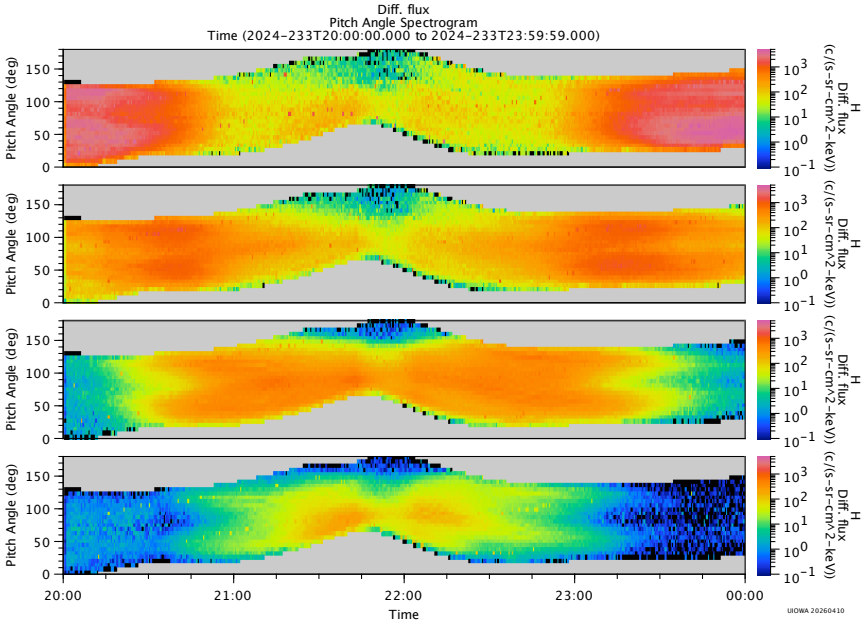

Figure 5: Proton PADs using the TOFxPH products. Each panel, starting from the top is (a) 23 keV, (b) 55 keV, (c) 152 keV, and (d) 478 keV.

Figure 6 shows the JoEE electron intensity energy spectrogram starting at 18:00 UTC on 20 August 2024 when JUICE entered the plasma sheet around midnight magnetic local time (MLT). There is a weak intensification between 18:00 and 19:00 UTC with slight energy dispersion, which is consistent with a weak excursion in the AE index starting just before 18:00 UTC and reaching a maximum of about 400 nT at around 18:10 UTC. Between 19:00 and 20:00 UTC there is an energy-dispersed feature (left leaning) where higher energy electrons reach the spacecraft before lower energy electrons and is therefore likely an injection originating at the earlier MLTs since electrons drift eastward. The broad feature in the 20:00-21:00 UTC period is consistent with a relatively fresh outer radiation belt population and the feature at higher energies centered around 1 MeV and 21:00 UTC is consistent with an older, remnant population in the outer radiation belt. The drop-out around closest approach in the 21:30-22:30 UTC period is the characteristic slot region, where high-energy electrons resonate with plasmaspheric hiss and scatter in to the atmosphere. See several past observations including Reeves et al. (2016) and references therein.

https://doi.org/10.5194/egusphere-2026-2050
Preprint. Discussion started: 15 April 2026

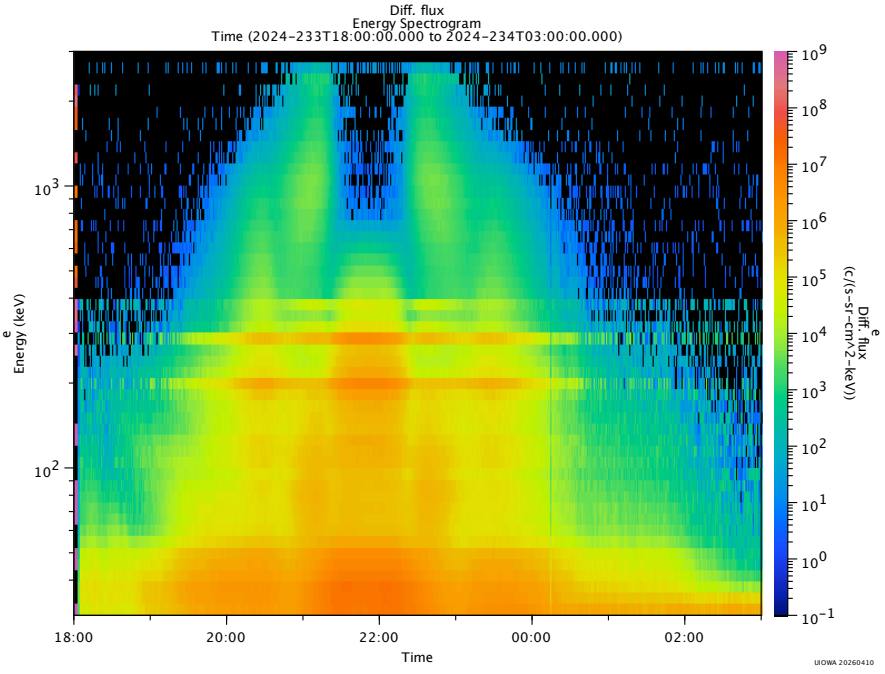

Figure 6: JoEE electron energy spectrogram showing the outer radiation belt with a double structure, and the slot region created by resonant pitch-angle scattering by plasmaspheric hiss. The horizontal streaks of higher intensities stem from mismatches in detector efficiencies.

3.3 Remote JENI ENA Observations

JENI switched to ENA mode at 00:14 UTC on 21 August 2024, while JoEE remained on in its standard science mode. Here, we provide an overview of the JENI ENA observations in this section and do not describe the JoEE observations as the energetic electron intensities in the solar wind were at or near detection threshold for JoEE. We refer to Dialynas et al. (2026, this issue) for a more detailed analysis of the JENI ENA image sequence.

Figure 7 shows a sequence of H ENA images, each integrated for 30 min over the 15-84 keV range. The angular pixel size of the data product is 2˚ and a smoothing function has been applied to the images to better aide interpretation. At this time the deflection voltage was set to 1.0 kV, which deflects protons only up to about 20 keV. However, the foreground ion intensities outside the terrestrial magnetosphere were lower than the ENA intensity. The first image Figure 6a is obtained at 04:15 UTC on 21 August 2024 at a geocentric distance of 17.4 R_E. The dayside is on the left with north pointing up. There are four sets of geomagnetic dipole field lines for reference at local times 00:00 (rightmost in the image), 06:00 (on the other side of Earth), 12:00 (leftmost in the image), and 18:00 (on this side of the Earth). Each set consists of L-shell 4 and 8, so that its intersection with the equatorial plane is 4 and 8 R_E, respectively. The vantage point is slightly below the magnetic equator so the viewer is looking “up” at the ring current slightly from southern latititudes. The emissions appear around

https://doi.org/10.5194/egusphere-2026-2050
Preprint. Discussion started: 15 April 2026

Earth in an almost symmetric fashion and is consistent with symmetric ring current as observed previously by the High-Energy Neutral Atom (HENA) camera onboard the IMAGE mission (Brandt et al. 2022).

Despite this being a relatively quiet period, JENI subsequently observed multiple intensifications on the night side throughout the observation period, which ended at the end of 23 August 2024 at a distance of 150 R_E. Figure 6b shows slightly more enhanced night side emissions at 09:00 UTC on 21 August (28.1 R_E) that was followed by a larger intensification peaking at around 13:00 UTC (36.7 R_E) in the center panel Figure 7c. In this particular image, the near-equatorial vantage point of JUICE offers a meridional view of the night side trapped proton population following the general shape of the dipole field lines. The emission morphology is slightly more elongated than the dipole shape, which is expected due to the stretched magnetic field on the night side. The general dominance of emissions in the south (below Earth) is a viewing effect caused by two physical mechanisms. First, the near-earth emissions from low altitudes are caused by nearly mirroring ions charge exchange with the neutral oxygen of the upper atmosphere (Roelof 1997; Brandt et al. 2001; Goldstein et al. 2018). These low-altitude emissions can be orders of magnitude stronger than the higher-altitude emissions further from Earth. The Point-Spread Function (PSF) of JENI is between 2˚ and 4˚ Full Width at Half Maximum (FWHM) above 15 keV H. This means that a very intenste point source, such as a 2˚ pixel containing low-altitude emission can bleed across almost a grid cell as depicted by the dashed latitude and longitude lines in the images. The second cause for the general dominance of emissions in the south is the more rounded PADs in the off-equator extensions of the magnetic field lines that create ENAs anisotropically. These viewing effects make direct detailed interpretion complex and is best handled by forward models or inversions (Roelof et al. 2000; DeMajistre et al. 2004; Brandt et al. 2022).

The remaining images in Figure 7 show other intensifications interleaved with quiet, weaker periods. These intensifications are generally consistent with bursts of geomagnetic activity and substorms as indicated by the AE index available at https://wdc.kugi.kyoto-u.ac.jp/index.html. Substorm injections have been previously observed in ENAs and successfully correlated to the auroral substorm development, which is expected as ENAs are a direct product of the charge exchange between the hydrogen geocorona and the magnetospheric ions energized in the substorm injection process (Mitchell et al. 2003; Brandt et al. 2002).

https://doi.org/10.5194/egusphere-2026-2050
Preprint. Discussion started: 15 April 2026

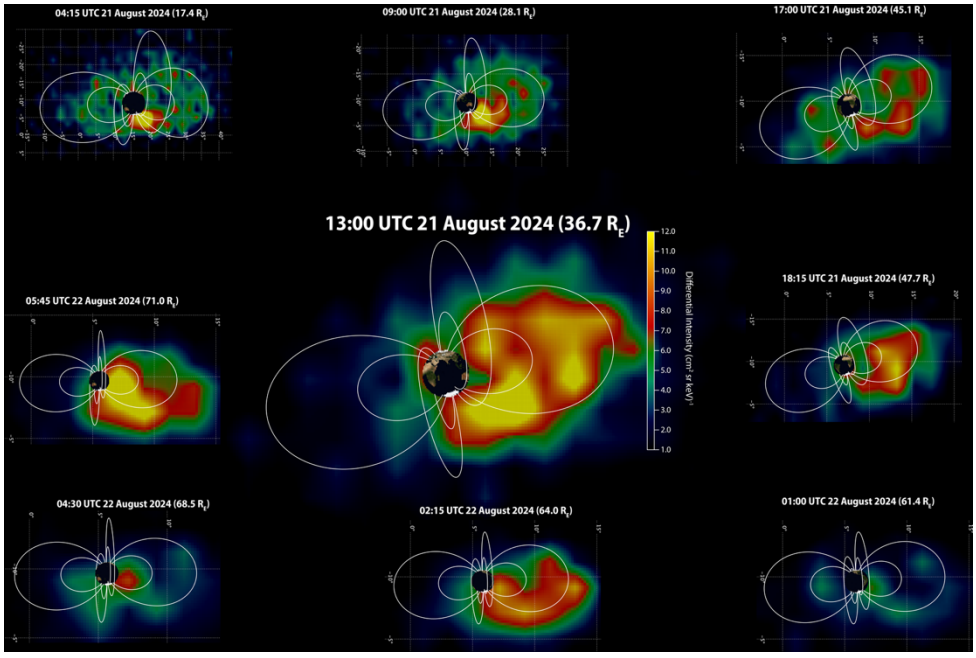

Figure 7: ENA image sequence from 04:15 UTC on 21 August to 05:45 UTC on 22 August showing several substorm intensifications with more quiet periods in between. See text and Dialynas et al. (2026, this issue) for more details.

Code and data availability

Data will become publicly available in the NASA Planetary Data System and ESA Planetary Science Archive at a later date. Until then, any data requests should be directed to the corresponding author.

Author contributions

Pontus C. Brandt led the overall development of the paper and its figures. Authors Donald G. Mitchell, Kostas Dialynas, and Matina Gkioulidou have provided in-depth analysis of the JENI, while authors George Clark and Peter Kollmann provided in-depth analysis of the JoEE data. Authors Stas Barabash and Peter Wurz have provided overall guidance as PEP Principal Investigator (PI) and Co-PI. Remaining authors have performed the review of the scientific results and the manuscript.

Competing interests

At least one of the (co-)authors is a member of the editorial board of Annales Geophysicae.

Acknowledgements

Special thanks to ESA JUICE Project and Airbus teams for excellent team work and comraderie making JUICE a success. This work was performed under NASA Task Order 80MSFC23F0077 under Contract 80MSFC20D0004 (ARDES II). French co-authors acknowledge the support of CNES for the Juice mission.

https://doi.org/10.5194/egusphere-2026-2050
Preprint. Discussion started: 15 April 2026

4 References

Barabash, S., P. Wurz, and P. C. Brandt. 2026. 'The Particle Environment Package (PEP) Onboard the Jupiter Icy Moon Explorer (JUICE)', *Space Science Reviews*.

Brandt, P. C., R. Demajistre, E. C. Roelof, S. Ohtani, D. G. Mitchell, and S. Mende. 2002. 'IMAGE/high-energy energetic neutral atom: Global energetic neutral atom imaging of the plasma sheet and ring current during substorms', *Journal of Geophysical Research: Space Physics (1978–2012)*, 10.1029/2002JA009307, http://dx.doi.org/10.1029/2002JA009307, 107.

Brandt, Pontus, Stas Barabash, Edmond C. Roelof, and Christopher J. Chase. 2001. 'Energetic neutral atom imaging at low altitudes from the Swedish microsatellite Astrid: Extraction of the equatorial ion distribution', *Journal of Geophysical Research: Space Physics*, 10.1029/2000ja900023, http://dx.doi.org/10.1029/2000ja900023, 106: 25731-44.

Brandt, Pontus C., Romina Nikoukar, Robert DeMajistre, Robert C. Allen, Donald G. Mitchell, Edmond C. Roelof, Malamati Gkioulidou, and Charles W. Parker. 2022. 'Chapter 2 - Energetic neutral atom imaging of the terrestrial global magnetosphere.' in Yaireska Colado-Vega, Dennis Gallagher, Harald Frey and Simon Wing (eds.), *Understanding the Space Environment through Global Measurements* (Elsevier).

Clark, G., P. Kollmann, and P. C. Brandt. 2026. 'JoEE Observations and Performance of the Terrestrial Radiation Belt During JUICE LEGA'.

DeMajistre, R., E. C. Roelof, P. C. Brandt, and D. G. Mitchell. 2004. 'Retrieval of global magnetospheric ion distributions from high-energy neutral atom measurements made by the IMAGE/HENA instrument', *Journal of Geophysical Research: Space Physics (1978–2012)*, 10.1029/2003ja010322, http://dx.doi.org/10.1029/2003ja010322, 109.

Futaana, Yoshifumi, Stas Barabash, Mats Holmström, and Anil Bhardwaj. 2006. 'Low energy neutral atoms imaging of the Moon', *Planetary and Space Science*, https://ui.adsabs.harvard.edu/abs/2006P&SS...54..132F, 54: 132-43.

Gkioulidou, M., D. G. Mitchell, G. Clark, and P. C. Brandt. 2026. 'JENI ENA Observations and Performance of the Terrestrial Ring Current During JUICE LEGA'.

Gloeckler, G., B. Wilken, W. Stüdemann, F. M. Ipavich, D. Hovestadt, D. C. Hamilton, and G. Kremser. 1985. 'First composition measurement of the bulk of the storm-time ring current (1 to 300 keV/e) with AMPTE-CCE', *Geophysical Research Letters*, 10.1029/gl012i005p00325, http://dx.doi.org/10.1029/gl012i005p00325, 12: 325-28.

Goldstein, J., K. LLera, D. J. McComas, J. Redfern, and P. W. Valek. 2018. 'Empirical Characterization of Low-Altitude Ion Flux Derived from TWINS', *Journal of Geophysical Research (Space Physics)*, 10.1029/2017ja024957, https://ui.adsabs.harvard.edu/abs/2018JGRA..123.3672G, 123: 3672.

Hamilton, D. C., G. Gloeckler, F. M. Ipavich, W. Stüdemann, B. Wilken, and G. Kremser. 1988. 'Ring current development during the great geomagnetic storm of February 1986', *Journal of Geophysical Research: Space Physics*, 10.1029/ja093ia12p14343, http://dx.doi.org/10.1029/ja093ia12p14343, 93: 14343-55.

Krimigis, S. M., D. G. Mitchell, D. C. Hamilton, S. Livi, J. Dandouras, S. Jaskulek, T. P. Armstrong, J. D. Boldt, A. F. Cheng, G. Gloeckler, J. R. Hayes, K. C. Hsieh, W. -H. Ip, E. P. Keath, E. Kirsch, N. Krupp, L. J. Lanzerotti, R. Lundgren, B. H. Mauk, R. W. McEntire, E. C. Roelof, C. E. Schlemm, B. E. Tossman, B. Wilken, and D. J. Williams. 2004. 'Magnetosphere Imaging Instrument (MIMI) on the Cassini Mission to Saturn/Titan', *Space Science Reviews*, https://ui.adsabs.harvard.edu/abs/2004SSRv..114..233K, 114: 233-329.

McComas, D. J., F. Allegrini, P. Bochsler, P. Frisch, H. O. Funsten, M. Gruntman, P. H. Janzen, H. Kucharek, E. Möbius, D. B. Reisenfeld, and N. A. Schwadron. 2009. 'Lunar backscatter and neutralization of the solar wind: First observations of neutral atoms from the Moon', *Geophysical Research Letters*, 10.1029/2009gl038794, http://dx.doi.org/10.1029/2009gl038794, 36.

Mitchell, D. G., S. E. Jaskulek, C. E. Schlemm, and Keath - E. P. Image …. 2000. 'High energy neutral atom (HENA) imager for the IMAGE mission', *The IMAGE …*, https://link.springer.com/chapter/10.1007/978-94-011-4233-5_4.

Mitchell, Donald G., Pontus Brandt, Edmond C. Roelof, Douglas C. Hamilton, Kyle C. Retterer, and Steven Mende. 2003. 'Global imaging of O+ from IMAGE/HENA', *Space Science Reviews*, 10.1023/b:spac.0000007513.55076.00, http://dx.doi.org/10.1023/b:spac.0000007513.55076.00, 109: 63-75.

Nosé, M., S. Taguchi, K. Hosokawa, S. P. Christon, R. W. McEntire, T. E. Moore, and M. R. Collier. 2005. 'Overwhelming O+ contribution to the plasma sheet energy density during the October 2003 superstorm: Geotail/EPIC and

https://doi.org/10.5194/egusphere-2026-2050
Preprint. Discussion started: 15 April 2026

IMAGE/LENA observations', *Journal of Geophysical Research: Space Physics (1978–2012)*, 10.1029/2004ja010930, http://dx.doi.org/10.1029/2004ja010930, 110.

Reeves, Geoffrey D., Reiner H. W. Friedel, Brian A. Larsen, Ruth M. Skoug, Herbert O. Funsten, Seth G. Claudepierre, Joseph F. Fennell, Drew L. Turner, Mick H. Denton, Harlan E. Spence, J. Bernard Blake, and Daniel N. Baker. 2016. 'Energy-dependent dynamics of keV to MeV electrons in the inner zone, outer zone, and slot regions', *Journal of Geophysical Research: Space Physics*, https://doi.org/10.1002/2015JA021569, https://agupubs.onlinelibrary.wiley.com/doi/abs/10.1002/2015JA021569, 121: 397-412.

Roelof, E. C. 1997. 'ENA emission from nearly-mirroring magnetospheric ions interacting with the exosphere', *Advances in Space Research*, 10.1016/s0273-1177(97)00692-3, http://dx.doi.org/10.1016/s0273-1177(97)00692-3, 20: 361-66.

Roelof, Edmond C., and Andrew J. Skinner. 2000. 'Extraction of ion distributions from magnetospheric ENA and EUV images', *Space Science Reviews*, 10.1023/a:1005281424449, http://dx.doi.org/10.1023/a:1005281424449, 91: 437-59.

Schaufelberger, A., P. Wurz, S. Barabash, M. Wieser, Y. Futaana, M. Holmström, A. Bhardwaj, M. B. Dhanya, R. Sridharan, and K. Asamura. 2011. 'Scattering function for energetic neutral hydrogen atoms off the lunar surface', *Geophysical Research Letters*, 10.1029/2011gl049362, http://dx.doi.org/10.1029/2011gl049362, 38.

Shi, Run, Danny Summers, Binbin Ni, Jerry W. Manweiler, Donald G. Mitchell, and Louis J. Lanzerotti. 2016. 'A statistical study of proton pitch angle distributions measured by the Radiation Belt Storm Probes Ion Composition Experiment', *Journal of Geophysical Research: Space Physics*, https://doi.org/10.1002/2015JA022140, https://agupubs.onlinelibrary.wiley.com/doi/abs/10.1002/2015JA022140, 121: 5233-49.

Vorburger, A., P. Wurz, S. Barabash, M. Wieser, Y. Futaana, C. Lue, M. Holmström, A. Bhardwaj, M. B. Dhanya, and K. Asamura. 2013. 'Energetic neutral atom imaging of the lunar surface', *Journal of Geophysical Research: Space Physics*, 10.1002/jgra.50337, http://dx.doi.org/10.1002/jgra.50337, 118: 3937-45.

Wieser, Martin, Stas Barabash, Yoshifumi Futaana, Mats Holmström, Anil Bhardwaj, R. Sridharan, M. B. Dhanya, Audrey Schaufelberger, Peter Wurz, and Kazushi Asamura. 2010. 'First observation of a mini-magnetosphere above a lunar magnetic anomaly using energetic neutral atoms', *Geophysical Research Letters*, 10.1029/2009gl041721, http://dx.doi.org/10.1029/2009gl041721, 37.

Wieser, Martin, Stas Barabash, Yoshifumi Futaana, Mats Holmström, Anil Bhardwaj, R. Sridharan, M. B. Dhanya, Peter Wurz, Audrey Schaufelberger, and Kazushi Asamura. 2009. 'Extremely high reflection of solar wind protons as neutral hydrogen atoms from regolith in space', *Planetary and Space Science*, 10.1016/j.pss.2009.09.012, http://dx.doi.org/10.1016/j.pss.2009.09.012, 57: 2132-34.